

## Comparative Study of Wavelet-SARIMA and Wavelet- NNAR Models for Groundwater Level in Rajshahi District

Md. Abdul Khalek\* and Md. Ayub Ali\*

\* Department of Statistics, University of Rajshahi, Rajshahi-6205, Bangladesh.

---

**Abstract:** This study compared the application of time series methods for forecasting groundwater levels at nine upazila's in Rajshahi district, Bangladesh. Accurate and reliable groundwater level forecasting models can help ensure the sustainable use of groundwater. A new method was proposed for forecasting groundwater level by combining the wavelet technique with seasonal autoregressive integrated moving average (SARIMA) and neural network autoregressive (NNAR) model applied to monthly groundwater level. The data were divided into a training dataset (January, 1991 to December, 2009) to construct the models and a testing dataset (January, 2010 to December, 2013) to estimate their performance. The relative performance of the proposed joined wavelet-seasonal autoregressive integrated moving average (W-SARIMA) and joined wavelet-neural network autoregressive (W-NNAR) models was compared to regular SARIMA and NNAR models for monthly groundwater level forecasting. The calibration and validation performance of the models is evaluated statistically, and the relative performance based on the predictive ability of out-sample forecasts is evaluated. The results indicate that the W-SARIMA model is more effective than the W-NNAR model, regular SARIMA and NNAR models.

**Keywords:** Groundwater Level Forecasting; Rajshahi District; W-SARIMA; W-NNAR

---

### I. Introduction

Water is the tonic of life and is crucial for sustainable development. Earlier, it was considered to be a limitless or at least fully renewable natural resource, but in the recent past, there has been a tremendous pressure on this valuable natural resource mainly due to rapid industrialization, population growth and using dimensionality of water. For an effective management of groundwater, it is important to predict groundwater level fluctuations. Groundwater systems possess features such as complexity, nonlinearity, being multi-scale and random, all governed by natural and/or anthropogenic factors, that complicates the dynamic predictions. Keeping in mind the scarcity of available water resources in the near future and its impending threats, it has become imperative on the part of water scientists as well as planners to quantify the available water resources for its judicial use. Thus, a ready reckoner to monitor the fluctuations in groundwater levels well in advance is the need of the hour to formulate and model the sustainable water management protocols.

At the present, there are many groundwater modeling approaches have been applied to forecast groundwater level and its fluctuations, within which, conceptual and physically based models; are the main types, for depicting hydrological variables and characterizing the complex structures of aquifers. Nevertheless, these modeling approaches do have some limitations in practice; for instance, a large number of accurate data (Mohammadi, 2006) is necessary for modeling. Autoregressive moving average (ARIMA) model is one of empirical models with its particular properties allowing generalizations of the process being analyzed. It is a linear prediction method which assumes that the present data is a function of past data and errors (Faruk, 2010). However, the performance and accuracy of the ARIMA model are not always satisfactory, it is also not adequate to apply ARIMA model to forecast groundwater level as the climate and exploitation changes over time greatly. The variation of groundwater level is highly nonlinear because of interdependencies and uncertainties in the hydrogeological process (Suryanarayani et al., 2014). Artificial intelligence techniques have been proved to be the effective methods in virtually modeling for any nonlinear function. To sum up, artificial neural networks (ANNs) and seasonal autoregressive integrated moving average (SARIMA) techniques are all widely used for predicting groundwater level at present, and all these techniques have been proved to be effective methods (Daliakopoulos et al., 2005; Krishna et al., 2008; Adamowski and Chan, 2011). The NNAR model is a relatively innovative method which is computer intensive and generally yields satisfactory results in terms of in-sample and out-of-sample measures after some proper *fine tuning* of its parameters. It is important not to apply neural network models blindly in "black box" mode but rather to select the parameters of the neural network model wisely by means of traditional modeling skills (Faraway. and Chatfield, 1998). All these models should have been being compared and to be highlighted the better one.

Thus, the purpose of this study is to build up several models SARIMA, NNAR and wavelet groundwater level time series data to forecast monthly groundwater level, and to compare their performances among the existing models.

## II. Study Area And Data Collection

We used secondary data as per requirements of modeling and forecasting of groundwater levels for northwest region of Bangladesh. Monthly time series data of groundwater level (GWL) from 1991 to 2013 were collected from Bangladesh Water Development Board (BWDB). Rajshahi, the northwestern administrative district of Bangladesh, is located at  $24.163^{\circ}\text{N}$  latitude and  $88.40^{\circ}\text{E}$  longitude. The northwestern part of Bangladesh is an interesting study area for its natural beauties of Barind track. Monthly groundwater level varies seasons to season, including the Rajshahi district and the neighboring district (Fig. 1), were collected from the Bangladesh Meteorological Department (BMD), which is the authorized government organization for meteorological activities in Bangladesh.

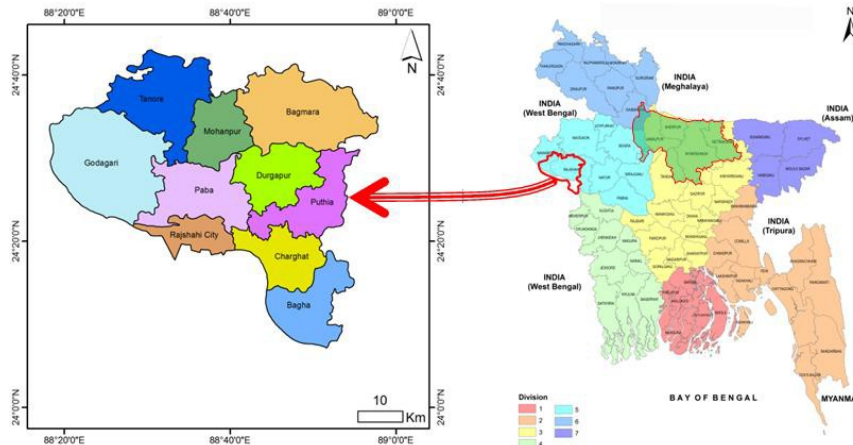


Fig. 1: Study area with locations of groundwater observation wells

## III. Methodology

### 3.1 Groundwater Level: Statistical Features

Besides wavelet features, we employed some additional features to represent the characteristics of time series. Five of them, i.e. Minimum, maximum, Mean, standard deviation (SD) and coefficient of variation (CV), are basic descriptive statistical measures that are commonly used in hydrology. In the proposed model, we use them to describe the data inside the time-window.

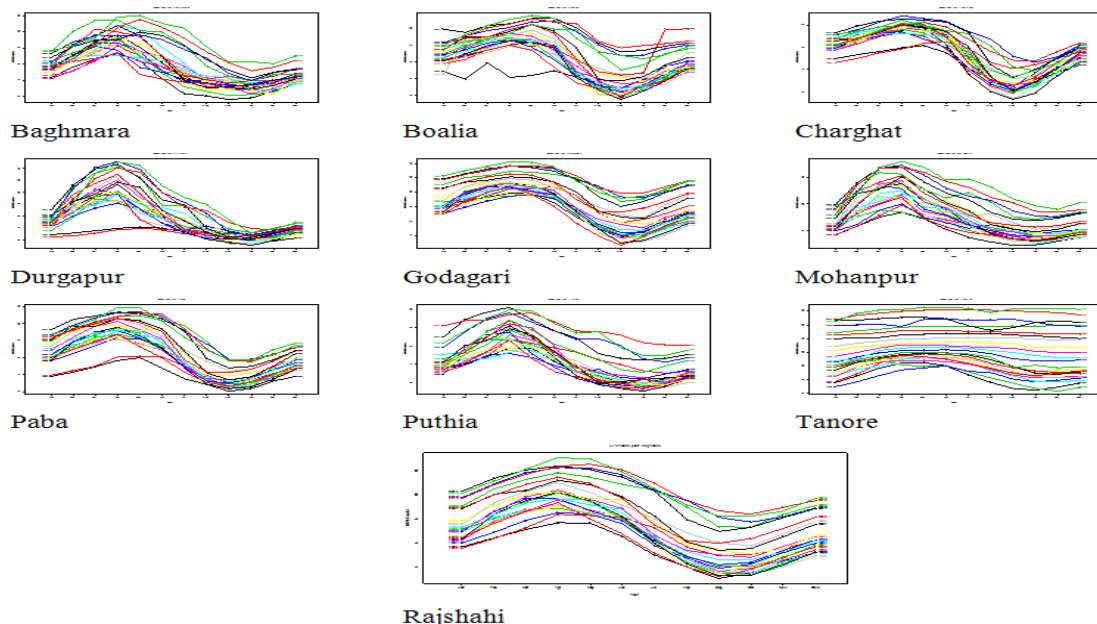


Fig. 2: Month-wise fluctuation of groundwater level in Rajshahi district

The table 1 presents groundwater level variation in my study area, from the following table GWL varies 1.07 meter to 18.55 meter. From Fig. 2, it is clearly state that the maximum groundwater level fluctuate in

March to May and minimum in September to November. This scenario carries almost nine upazilas except Tanore.

**Table 1.** Statistical parameters of input variables by Upazila/District

Upazila/District	Training					Test				
	Minimum	Maximum	Mean	SD	CV	Minimum	Maximum	Mean	SD	CV
Baghmara	1.65	11.49	5.54	2.20	39.68	3.96	11.99	7.74	2.14	27.65
Boalia	1.52	10.50	6.07	2.27	37.33	6.38	11.51	9.03	1.51	16.74
Charghat	1.33	8.26	5.42	1.86	34.41	3.30	8.82	6.54	1.59	24.27
Durgapur	1.19	14.30	5.26	2.88	54.77	2.49	15.15	8.10	4.12	50.83
Godagari	2.66	12.91	8.14	2.52	30.99	8.04	14.24	11.72	1.67	14.22
Mohanpur	2.27	15.88	7.27	3.23	44.46	6.89	17.93	11.95	3.36	28.09
Paba	2.08	10.98	6.16	2.34	38.04	4.81	11.93	8.60	2.21	25.66
Puthia	1.07	8.86	4.06	1.88	46.17	4.26	10.24	7.25	1.76	24.31
Tanore	6.32	15.91	11.27	2.35	20.83	15.21	18.55	17.18	0.94	5.50
<b>Rajshahi</b>	<b>3.11</b>	<b>11.83</b>	<b>7.08</b>	<b>2.13</b>	<b>30.11</b>	<b>6.99</b>	<b>13.07</b>	<b>10.26</b>	<b>1.69</b>	<b>16.44</b>

### 3.2 Seasonal Autoregressive Integrated Moving Average (SARIMA)

The seasonal autoregressive integrated moving average (SARIMA) method can be used to identify complex patterns in data and to generate forecasts (Box and Jenkins, 1976). An SARIMA model predicts a value in a response time series as a linear combination of its own past values (Parnell, 2013). SARIMA models involve a combination of three types of processes: (1) an autoregressive (AR) process, (2) differencing to strip the integration (I), and (3) a moving average (MA) process. The general form of the SARIMA (p, d, q) model is

$$\phi_p(L)(1 - L)^d Y_t = \theta_0 + \theta_q(L)U_t \quad \dots \dots \dots (1)$$

where  $\theta_0$  represents the intercept term,  $\phi_p(L)$  represents the AR part ( $1 - \phi_1L - \dots - \phi_pL^p$ ),  $\theta_q(L)$  represents the MA part ( $1 - \theta_1L - \dots - \theta_qL^q$ ), and  $U_t$  represent a zero mean white process with constant variance. Seasonal autoregressive integrated moving average (SARIMA) is a popular linear model for predicting seasonal time series. A time series  $\{Z_t | 1, 2, \dots, k\}$  is created by the SARIMA process of Box and Jenkins time series modeling [Box and Jenkins, 1976] if:

$$\phi_p(B)\phi_P B^S(1 - B)^d(1 - B^S)^D Z_t = \theta_q(B)\Theta_Q(B^S) \quad \dots \dots \dots (2)$$

Where p, d, q, P, D, Q are integers, s is the season length:

$$\phi_p(B) = 1 - \phi_1(B) - \phi_2 B^2 - \dots - \phi_p B^p \quad \dots \dots \dots (3)$$

$$\phi_P(B^S) = 1 - \phi_s B^S - \phi_{2s} B^{2s} - \dots - \phi_{Ps} B^{Ps}$$

$$\theta_q(B) = 1 - \theta_1 B - \theta_2 B^2 - \dots - \theta_q B^q$$

$$\Theta_Q(B^S) = 1 - \Theta_s B^S - \Theta_{2s} B^{2s} - \dots - \Theta_{Qs} B^{Qs}$$

As polynomials in B, where B is the backwards transfer factor,  $\epsilon_t$  is the estimated residual at time t, d is the number of normal difference, D is the number of seasonal differences,  $Z_t$  indicates the observed value at time t,  $t = 1, 2, \dots, k$ .  $\epsilon_t$  is independently and definitely distributed as a normal random variable with mean 0 and constant variance  $\sigma^2$ . The roots of  $\phi_p(Z) = 0$  and  $\theta_q(Z) = 0$  are all situated outside the unit circle. Fitting a SARIMA model to data entails a four-step iterative process: (i) discerning the SARIMA (p, d, q) (P, D, Q) structure; (ii) estimating unknown parameters; (iii) carrying out goodness of-fit tests on the estimated residuals; and (iv) predicting future values based on the known data. The fitting of SARIMA models requires the use of autocorrelation function (ACF) charts.

### 3.3 The Neural Network Autoregression Model

Artificial neural networks allow the modeling of complex nonlinear relationships among input variables and output variables. In the case of a neural network autoregression model (NNAR), lagged values of a time series are used as input to the model and the output are the predicted values of the time series. One of the main differences between the NNAR and the SARIMA method is that the NNAR does not impose any restriction on its parameters to ensure stationarity. In this paper we shall use the notation  $NNAR(p, P, k)_m$  proposed by Hyndman, and Athanasopoulos (2014) due to the seasonal component present in the monthly groundwater level. The structure of the  $NNAR(p, P, k)_m$  is represented in Fig. 3.

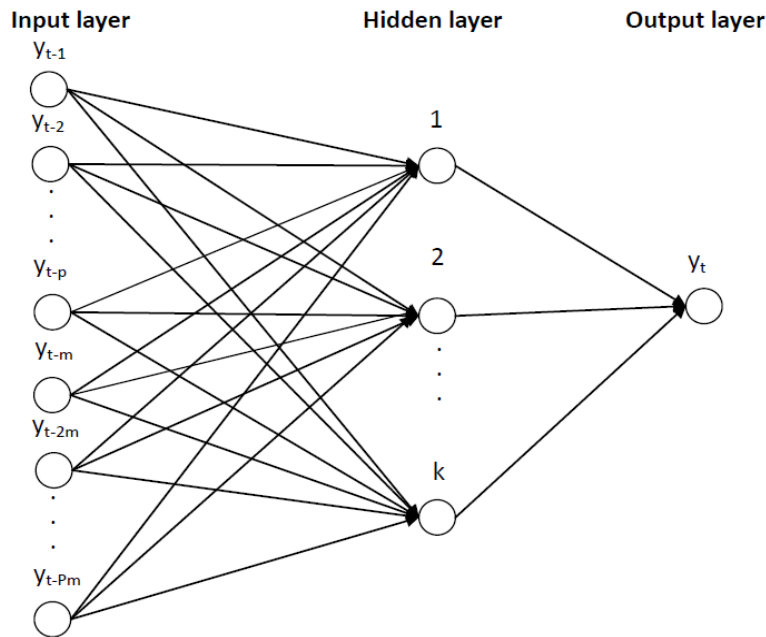


**Fig.3:** A diagrammatic representation of the NNAR( $p, P, k$ )<sub>m</sub> model

In the absence of a hidden layer, the NNAR( $p, P, 0$ )<sub>m</sub> is analogous to the SARIMA model denoted as an ARIMA( $p, 0, 0$ )( $P, 0, 0$ )<sub>m</sub>. Faraway and Chatfield (1998) suggest that to apply a good neural network model, a combination of traditional modeling skills with knowledge of time series is essential.

To ensure that a good artificial neural network model be fit, it is crucial to understand the idiosyncrasies of the monthly groundwater levels data. It is clear that there is a periodic component of  $m=12$  for the monthly groundwater level (GwL) data which relates to a seasonal effect. The NNAR model is a feedforward neural network which involves a linear combination function and an activation function. The linear combination function is generally formulated as

$$net_j = \sum_i w_{ij}y_{ij} \quad \dots (4)$$

although in some cases an intercept term is generally included. The activation function is a sigmoid function defined as

$$f(y) = \frac{1}{1 + e^{-y}} \quad \dots (5)$$

The inputs are combined through the linear function and the result of the combination is then passed through the non-linear sigmoid activation function. In R Core Team (2014), the weights of the neural network are updated using the back propagation algorithm. Since the weights are obtained through computational procedure, it is not possible to interpret the weights like in the case of traditional regression models which involve a closed form for the minimization of sum of squared errors. Indeed, Faraway and Chatfield (1998) state that it is not advisable to interpret the fitted weights.

### 3.4 Wavelet analysis

Mathematical functions which serve in the analysis of non-stationary time series, wavelet transforms allow one to decompose time series into low frequency and high frequency information, thereby exposing trends, breakdown points, and discontinuities in the data that other signal analysis methods might miss [Adamowski et al. 2009; Nalley et al. 2013]. Another advantage of wavelet transforms is the flexibility of choice in selecting a mother wavelet according to the properties of the time series [Conraria, &Soares (2011); Pingale et al. 2014]. Wavelet analysis has developed a popular tool due to its capability to reveal evidence within the indication in both the time and scale domains (Nourani et al., 2009). This property overcomes the basic drawback of Fourier analysis, which is that the Fourier spectrum provides a comprehensive clarification of the properties of the non-stationary procedures by yielding a mapping that is localized in frequency but global in time (Pal and Devara, 2012). Wavelet analysis is a mathematical procedure that transforms the original motion into a different domain for analysis and processing (Dong et al., 2001). This model is appropriate for non-stationary data, i.e., where the mean and autocorrelation of the signal are not constant over time. Most climatic time series data are non-stationary; therefore, wavelet transforms are used for these kinds of data.

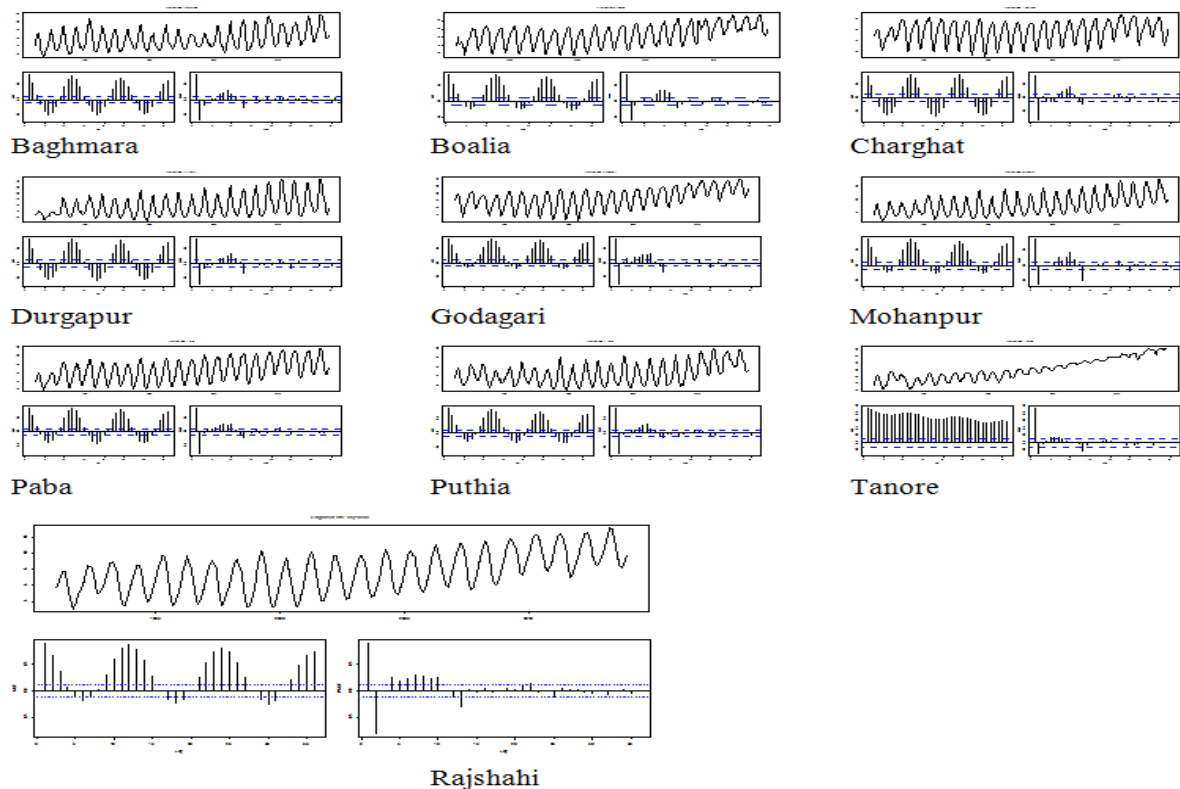


**Fig. 4:** Time series properties of monthly groundwater level in Rajshahi district.

Morlet first considered wavelets as a family of functions constructed from the translations and dilations of a single function, which is called the “*mother wavelet*”. Continuous wavelet analysis (CWT) represents the sum over all time of the signal, multiplied by scale and shifted versions of the mother wavelet analysis  $\psi$  [Kim and Valdes, 2003]:

$$\psi(\tau, s) = \frac{1}{\sqrt{|s|}} \int_{-\infty}^{+\infty} x(t) \psi^* \left( \frac{t - \tau}{s} \right) dt \quad \dots \dots \dots (6)$$

where,  $s$  is the scale parameter,  $t$  is time, and  $\tau$  is the shift parameter. Each scale corresponds to the width of the wavelet. While a CWT is useful in processing various images and signals, it is seldom used for prediction as its calculations are intricate and lengthy in terms of time. As an alternative, in prediction applications, the discrete wavelet transform (DWT) is applied, due to its simplicity and shorter calculation time. The scales and shifts of the DWT are usually based on powers of two (dyadic scales and shifts). This is obtained by altering the wavelet transform:

$$\psi(m)_{j,m} = \frac{1}{\sqrt{|s_0^j|}} \sum_k \psi \left( \frac{k - m\tau_0 s_0^j}{s_0^j} \right) x(k) \quad \dots \dots \dots (7)$$

where,  $j$  and  $m$  are integers which control the scale and shift, respectively,  $s_0 > 1$  is a fixed expansion step, and  $\tau_0$  is a shift parameter based on the aforementioned expansion step. The impact of discretizing the wavelet transform is that the time-space scale is sampled at discrete levels. The DWT functions like a pair of high pass and low pass filters. The time series is decomposed into one comprising its trend (the approximation) and one comprising the high frequencies and the fast events (the details) [Adamowski, Sun 2010]. In the present study, the detail coefficients and approximation sub-time series were obtained using eq. (7).

**3.5 Joined wavelet and SARIMA (W-SARIMA) model**

Noise in the time series data will significantly affect the accuracy of the forecast because SARIMA methods cannot handle non-stationary data without preprocessing the input data. To solve this problem, a wavelet denoising-based model is proposed.

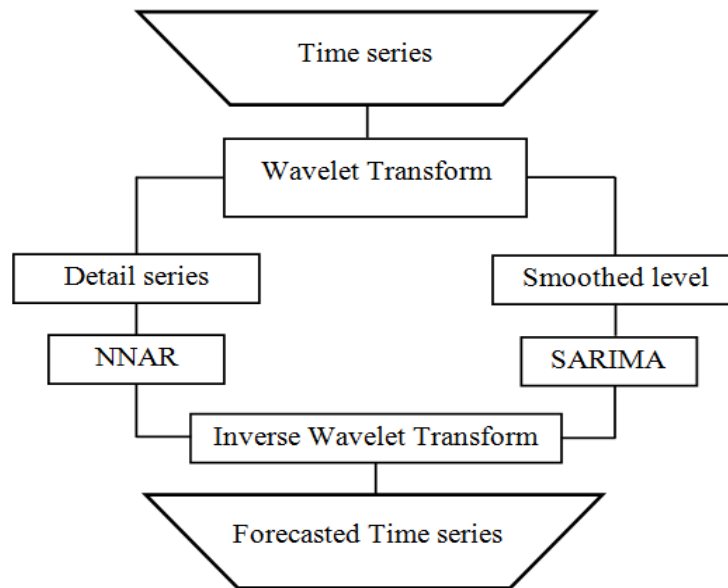


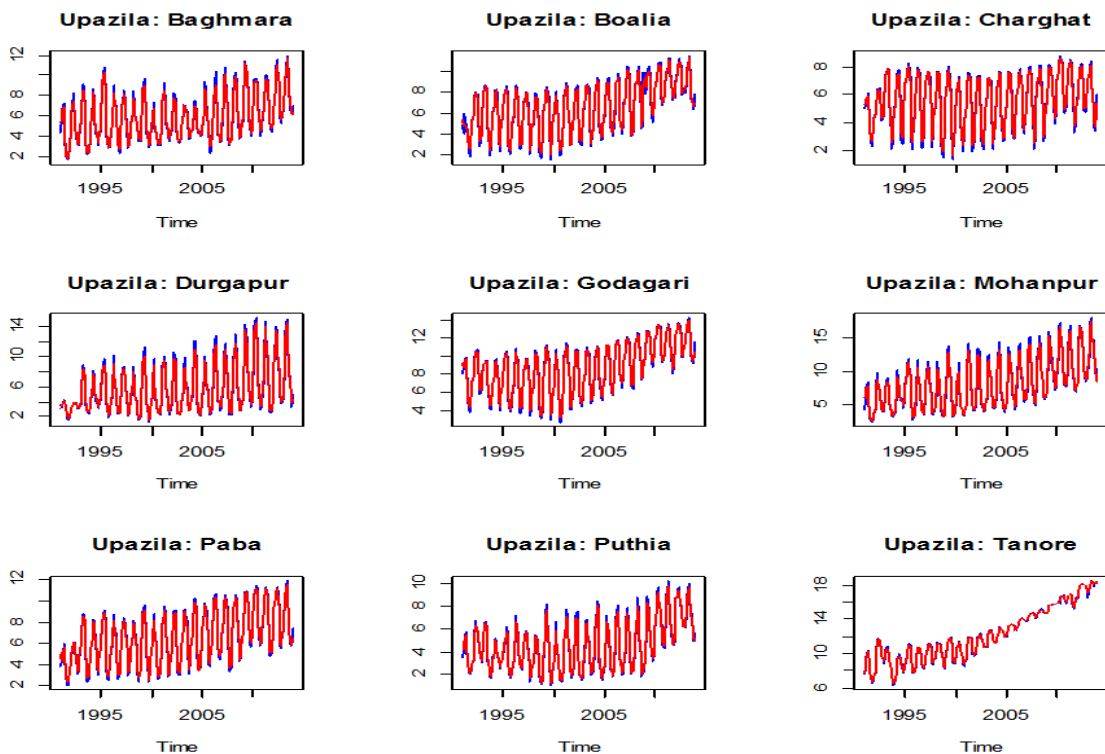
Fig. 5: Working structure of W-SARIMA model

When conducting wavelet analysis, the selection of the optimal number of decomposition levels is one of the keys to determine the performance of model in the wavelet domain. To select the number of decomposition levels, the following formula is used (Wang and Ding, 2003);

$$L = \text{int}[\log(N)] \quad \dots \dots \dots (8)$$

where, L and N are number of decomposition levels and time series length, respectively. For this study, N = 276; therefore, L ≈ 3. Kisi and Cimen (2011) used three decomposition levels in their monthly stream flow forecasting study. Several studies have obtained the best result using three decomposition levels.

The choice of mother wavelet depends on the data to be analyzed. Daubechies wavelets show a good trade-off between parsimony and information richness and identical events across the observed time series are produced by it in so many fashions that most prediction models cannot recognize them well (Reis and Silva, 2005). The procedure of W-SARIMA model is described as follows:



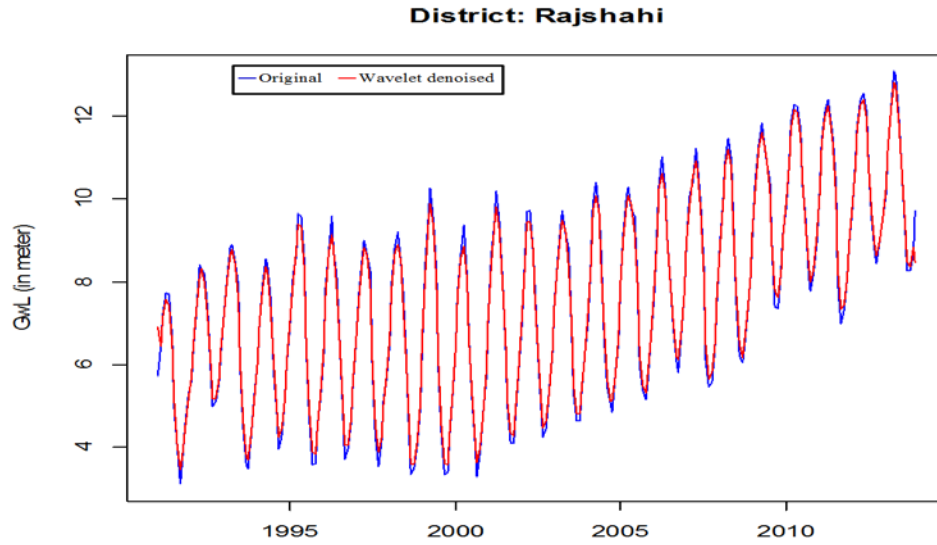


Fig. 6: Wavelet de-noised signal of groundwater level in Rajshahi district.

**Step 1:** The wavelet transformation, which is a Daubechies-5 type and a decomposition level 3, is applied. Application to the series  $Y_t$  ( $t = 1, 2, \dots, T$ ) results in 10 series, which are denoted by  $S3_t, D3_t, D2_t$  and  $D1_t$ ;  $t = 1, 2, \dots, T$ .  $WT(Y_t; t=1, 2, \dots, T) = \{S3_t, D3_t, D2_t, D1_t; t = 1, 2, \dots, T\}$ .

**Step 2:** The series is reconstructed by removing the high-frequency component, using the wavelet denoising method.

$$WT^{-1}\{S3_t, D3_t, D2_t; t = 1, 2, \dots, T\} = Y_t^*; t = 1, 2, \dots, T$$

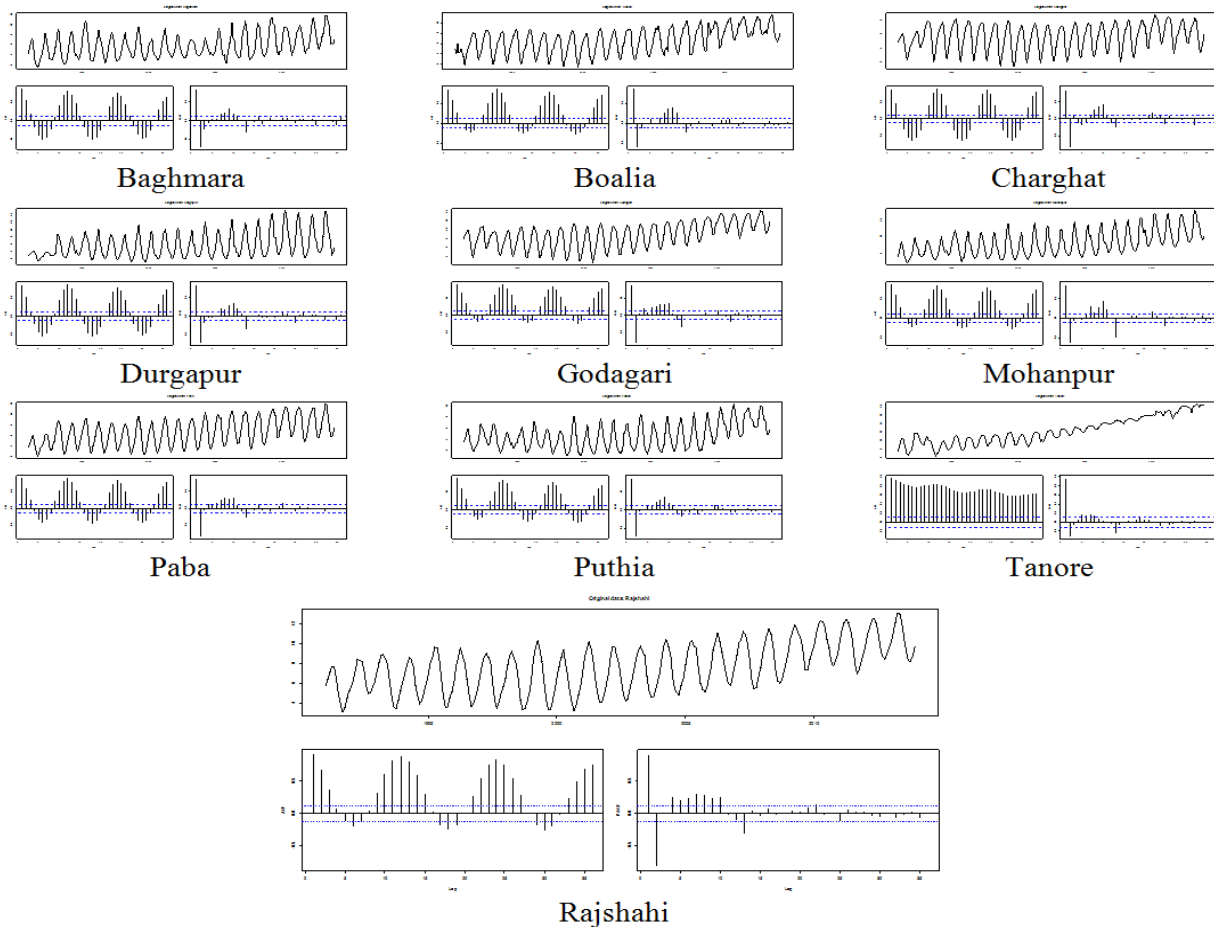


Fig. 7: Wavelet decomposition of groundwater level in Rajshahi district.

**Step 3:** The appropriate SARIMA model is applied to the reconstructed series to forecast the test series.

$$\{Y_t^*; t = 1, 2, \dots, T \xrightarrow{\text{SARIMA forecast}} Y_t^f; t = T + 1, \dots, T + n\}$$

**Table 2:** Augmented Dickey-Fuller (ADF) unit root test of original and wavelet denoised series.

Upazila/District	Include in test equation	Original series		Wavelet denoised series	
		ADF statistic	p-value	ADF statistic	p-value
Baghmara	Drift	-0.930	0.7776	-1.780	0.3900
	Drift and linear trend	-2.174	0.5019	-3.099	0.1087
	None	1.304	0.9515	0.677	0.8615
Boalia	Drift	-0.825	0.8100	-0.775	0.8239
	Drift and linear trend	-1.619	0.7830	-1.974	0.6123
	None	1.727	0.9798	0.743	0.8742
Charghat	Drift	-2.512	0.1137	-2.868	0.0505
	Drift and linear trend	-2.679	0.2462	-2.898	0.1650
	None	0.422	0.8038	-0.005	0.6803
Durgapur	Drift	-1.215	0.6685	-2.025	0.2761
	Drift and linear trend	-2.523	0.3167	-3.397	0.0540
	None	1.370	0.9573	0.834	0.8905
Godagari	Drift	-0.176	0.9383	-0.848	0.8033
	Drift and linear trend	-1.908	0.6478	-2.276	0.4452
	None	1.390	0.9589	0.510	0.8251
Mohanpur	Drift	-0.112	0.9457	-0.776	0.8236
	Drift and linear trend	-1.996	0.6003	-2.787	0.2034
	None	1.886	0.9860	1.084	0.9275
Paba	Drift	-1.336	0.6132	-2.198	0.2075
	Drift and linear trend	-2.789	0.2027	-2.815	0.1931
	None	1.468	0.9649	0.456	0.8123
Puthia	Drift	-0.253	0.9283	-1.595	0.4838
	Drift and linear trend	-1.408	0.8567	-2.542	0.3075
	None	1.178	0.9387	0.085	0.7090
Tanore	Drift	0.316	0.9788	0.962	0.9962
	Drift and linear trend	-2.109	0.5378	-2.370	0.3943
	None	2.459	0.9968	2.617	0.9980
Rajshahi	Drift	-0.051	0.9520	-1.193	0.6781
	Drift and linear trend	-1.872	0.6661	-2.313	0.4250
	None	1.757	0.9811	0.517	0.8268

**3.6 Joined wavelet and NNAR (W-NNAR) model**

A W-NNAR model was constructed in which the subseries  $\{D_1, D_2, D_3, S_3\}$  at time  $t$  are used as the inputs of the NNAR and the denoised time series at time  $t$  is the output of the NNAR network.

**Table 3:** Parameter estimation of de-noised SARIMA model for groundwater level

	Coeff±SE	AR1	AR2	AR3	MA1	MA2	SAR1	SAR2	SMA1	SMA2	SMA3
Baghmara	Coefficient	-0.080	0.611	-0.151	0.043	-0.957	-0.721	0.272	-0.033	-0.967	
	Std Error	0.078	0.066	0.072	0.039	0.039	0.101	0.081	0.159	0.156	
Boalia	Coefficient	1.432	-0.654		-1.691	0.749	0.758	0.206	-0.583		
	Std Error	0.111	0.102		0.099	0.106	0.144	0.129	0.136		
Charghat	Coefficient	0.586			-0.440	-0.464	0.192	0.134	-1.000		
	Std Error	0.086			0.088	0.066	0.079	0.086	0.109		
Durgapur	Coefficient	0.934	-0.169		-0.110		-0.256	-0.119	-0.436		
	Std Error	0.567	0.431		0.570		0.162	0.112	0.157		
Godagari	Coefficient	0.254	0.492	-0.155	-0.205	-0.696	1.690	-0.809	-2.529	2.257	-0.727
	Std Error	0.002	0.001	0.067	0.001	0.003	0.145	0.128	0.151	0.248	0.112
Mohanpur	Coefficient	-0.134	0.543		-0.071	-0.864	-0.990	-0.012	0.321	-0.610	
	Std Error	0.157	0.143		0.130	0.133	0.197	0.127	0.202	0.140	
Paba	Coefficient	0.450	0.117		-0.392	-0.479	0.049		-0.885	0.127	
	Std Error	0.242	0.215		0.220	0.215	0.469		0.460	0.365	
Puthia	Coefficient	0.023	-0.207				-0.115		-0.714		
	Std Error	0.070	0.067				0.094		0.076		
Tanore	Coefficient	1.502	-0.614		-1.305	0.341	0.928	0.032	-0.688		
	Std Error	0.131	0.123		0.154	0.149	0.104	0.093	0.088		
Rajshahi	Coefficient	<b>0.376</b>	<b>0.279</b>		<b>-0.279</b>	<b>-0.638</b>	<b>-0.474</b>	<b>-0.049</b>	<b>-0.334</b>	<b>-0.238</b>	
	Std Error	<b>0.209</b>	<b>0.190</b>		<b>0.177</b>	<b>0.177</b>	<b>3.398</b>	<b>0.584</b>	<b>3.405</b>	<b>2.188</b>	

The data set was then loaded and divided into two parts: training data (first 228 values of each data set) and testing data (subsequent 48 values of each data set). Employed delay lines were used for both the input and the output, so the training began with the next data point of the tapped delay line. The Levenberg-Marquardt

(LM) algorithm was utilized to train the NNAR models because it has been shown to be fast, accurate, and reliable (Adamowski and Karapataki, 2010).

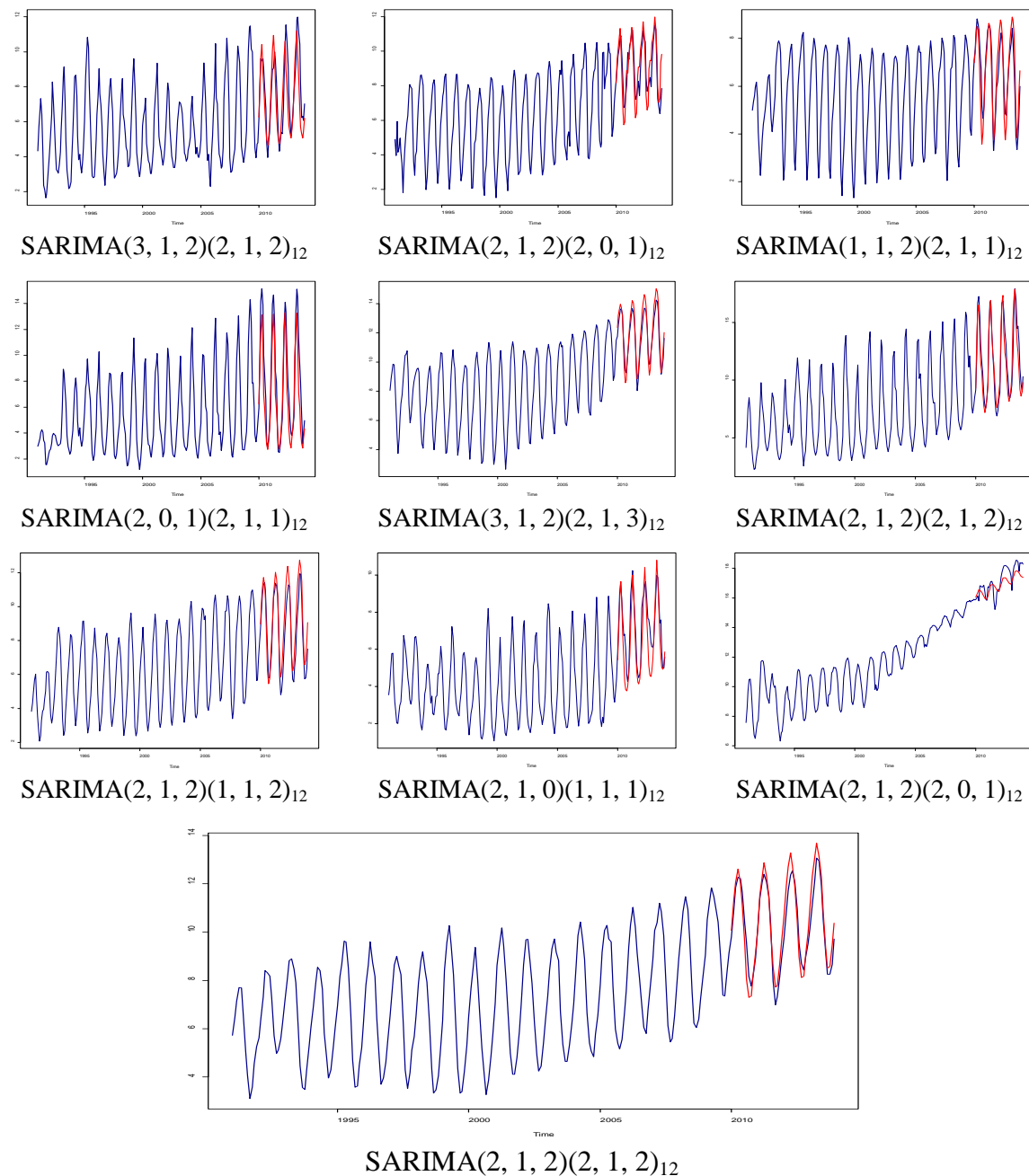


**Fig. 8:** In sample SARIMA forecast of groundwater level in Rajshahi district

To identify the optimal number of hidden neurons, a trial and error procedure was initiated with two hidden neurons, and the number of hidden neurons was increased to 20 with a step size of 1 in each trial (Ramana et al., 2013). For each set of hidden neurons, the network was trained in batch mode to minimize the mean square error of the output layer. To identify over fitting during the training, a cross validation step was performed by evaluating the efficiency of the fitted model. The training was stopped when there was no significant improvement in the efficiency, and the model was then used for its generalization properties (Ramana et al., 2013).

#### IV. Comparison Of Model Performance

Model performance was assessed using root mean square error (RMSE), percent of bias (PBIAS) and index of agreement (d). Root mean square error (Singh et al., 2005) is an estimate of the standard deviation of

the random components in the data, and the best model has a minimum RMSE. The percent of bias measures the average tendency of the simulated data to be larger or smaller than the observed counterparts.

$$ME = \frac{1}{n} \sum_{t=1}^n [Y_t(\text{Actual}) - Y_t(\text{Forecasted})] \quad \dots \dots \dots (8)$$

$$RMSE = \sqrt{\frac{\sum_{t=1}^n [Y_t(\text{Actual}) - Y_t(\text{Forecasted})]^2}{n}}$$

$$MPE = \left( \frac{1}{n} \sum_{t=1}^n \frac{Y_t(\text{Actual}) - Y_t(\text{Forecasted})}{Y_t(\text{Actual})} \right) \times 100\%$$

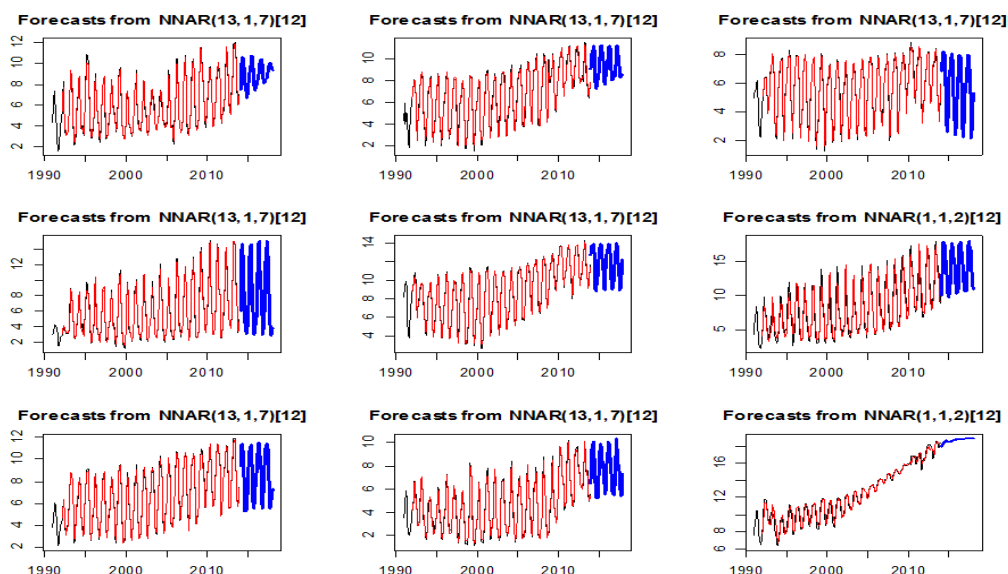
$$MAPE = \frac{1}{n} \sum_{t=1}^n \left| \frac{Y_t(\text{Actual}) - Y_t(\text{Forecasted})}{Y_t(\text{Actual})} \right|$$

**Table 4:** Accuracy of SARIMA model for original and wavelet de-noised groundwater level

Upazila/ District	SARIMA					Denoised-SARIMA				
	ME	RMSE	MAE	MPE	MAPE	ME	RMSE	MAE	MPE	MAPE
Baghmara	0.423	6.490	4.820	-8.740	91.500	-0.011	0.247	0.189	-0.557	3.695
Boalia	0.676	7.810	5.490	-14.800	108.000	-0.001	0.246	0.175	-0.315	3.090
Charghat	0.066	2.940	1.910	0.322	43.600	0.005	0.094	0.065	0.080	1.386
Durgapur	0.048	9.850	7.300	-14.400	152.000	0.001	0.230	0.168	-0.134	3.436
Godagari	0.328	3.890	2.930	1.300	40.600	0.007	0.129	0.095	0.109	1.288
Mohanpur	0.076	6.910	4.860	-11.300	67.000	-0.014	0.211	0.147	-0.343	1.987
Paba	-0.106	3.560	2.420	-6.600	41.300	0.005	0.183	0.135	-0.111	2.338
Puthia	-0.069	5.330	4.100	-18.800	112.000	0.011	0.155	0.113	0.179	2.983
Tanore	0.396	3.100	2.200	2.730	21.800	0.000	0.080	0.054	-0.010	0.527
<b>Rajshahi</b>	<b>-0.007</b>	<b>2.720</b>	<b>1.870</b>	<b>-1.770</b>	<b>27.300</b>	<b>0.001</b>	<b>0.072</b>	<b>0.051</b>	<b>0.013</b>	<b>0.719</b>

**Table 5:** Accuracy of NNAR model for original and wavelet de-noised groundwater level

Upazila/ District	NNAR					Denoised NNAR				
	ME	RMSE	MAE	MPE	MAPE	ME	RMSE	MAE	MPE	MAPE
Baghmara	0.003	4.321	3.230	-7.317	60.741	0.001	0.321	0.249	-1.540	4.858
Boalia	0.064	5.361	3.935	-28.987	81.722	0.000	0.270	0.207	-0.969	3.749
Charghat	0.005	2.694	1.983	-5.086	45.968	0.000	0.109	0.081	-0.072	1.720
Durgapur	0.034	6.222	4.580	-14.388	92.516	0.003	0.255	0.199	-1.521	4.338
Godagari	-0.002	7.320	5.729	-11.375	82.152	0.001	0.360	0.271	-0.250	3.640
Mohanpur	0.020	6.027	4.379	-6.706	59.987	-0.001	0.422	0.325	-0.357	4.528
Paba	0.002	3.554	2.702	-12.127	48.547	-0.001	0.256	0.212	-1.545	4.015
Puthia	-0.011	3.460	2.668	-10.384	75.180	0.000	0.142	0.110	-0.116	2.921
Tanore	0.012	4.448	3.256	-2.078	32.433	0.000	0.198	0.154	-0.046	1.485
<b>Rajshahi</b>	<b>0.005</b>	<b>4.361</b>	<b>3.335</b>	<b>-4.199</b>	<b>49.525</b>	<b>0.000</b>	<b>0.274</b>	<b>0.213</b>	<b>-0.177</b>	<b>3.123</b>



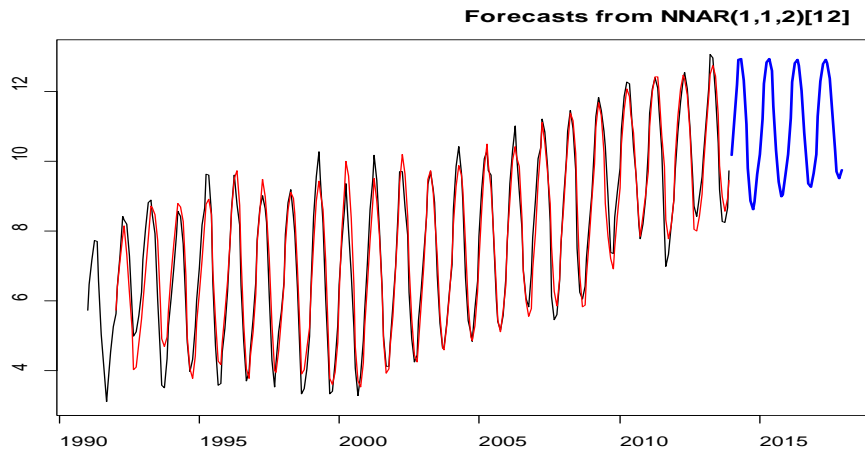


Fig. 9: Neural network performance curve of groundwater level in Rajshahi district

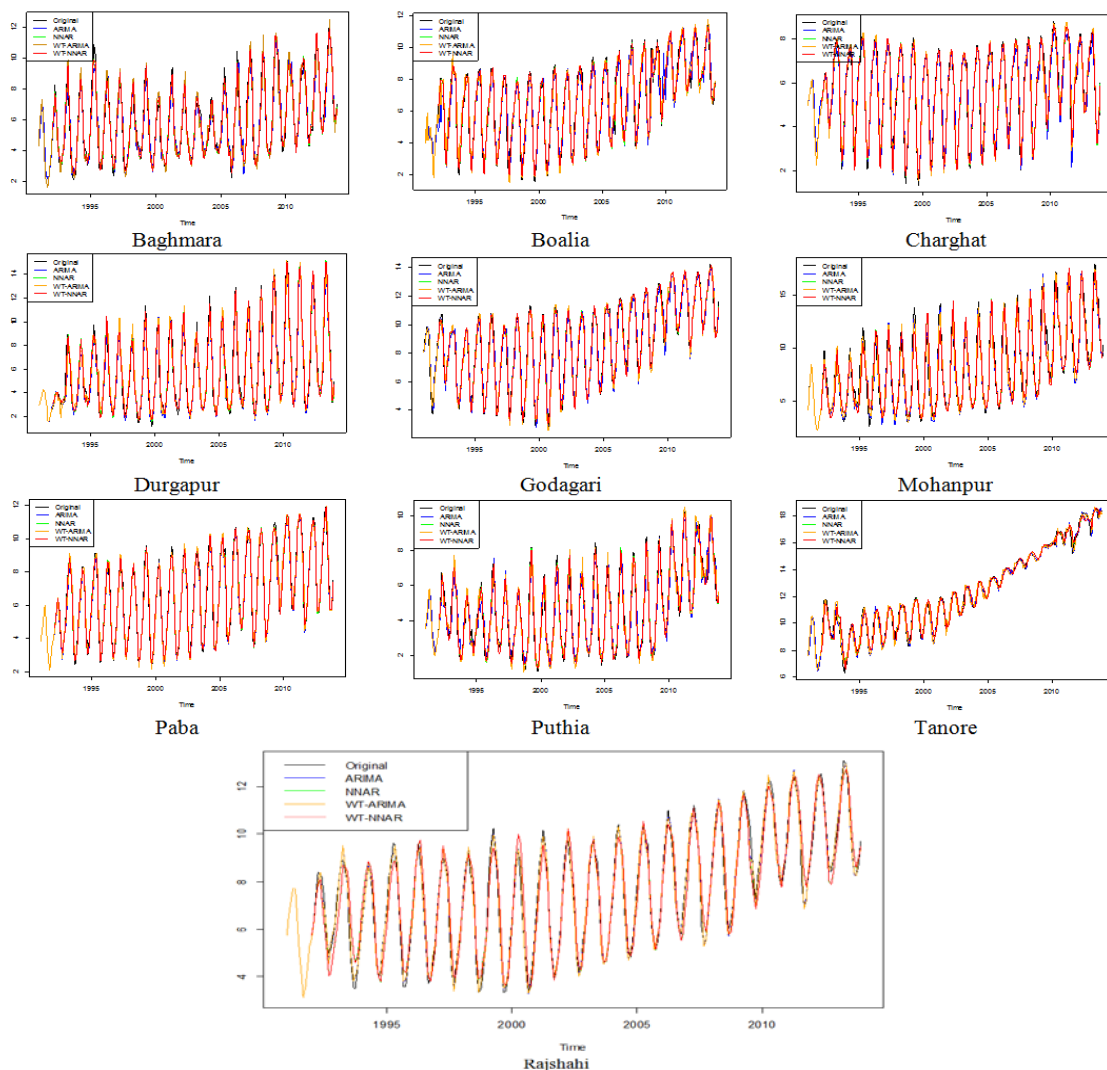


Fig. 10: Accuracy assessment of groundwater level models obtained using a W-SARIMA-NNAR model

## V. Results And Discussion

### 5.1 The SARIMA results

The SARIMA models for groundwater level forecasting for study sites were developed using the R software. Since the SARIMA method is a univariate time series analysis method, only one variable can be used (groundwater level). The first step is to determine the stationarity of the input data series via the autocorrelation

function (ACF). It was determined that the groundwater level data series were not stationary. The SARIMA model requires the input data to have a constant mean, variance, and autocorrelation through time. Therefore, the input data series were transformed into a stationary model through a differencing process. In the models that were developed, the number of autoregressive terms (p) varied from 0 to 5, and the number of lagged forecast errors in the prediction equation (q) varied from 0 to 5. All SARIMA models were first trained using the data in the training set (January 1991 to December 2009), and then tested using testing set (January 2010 to December 2013).

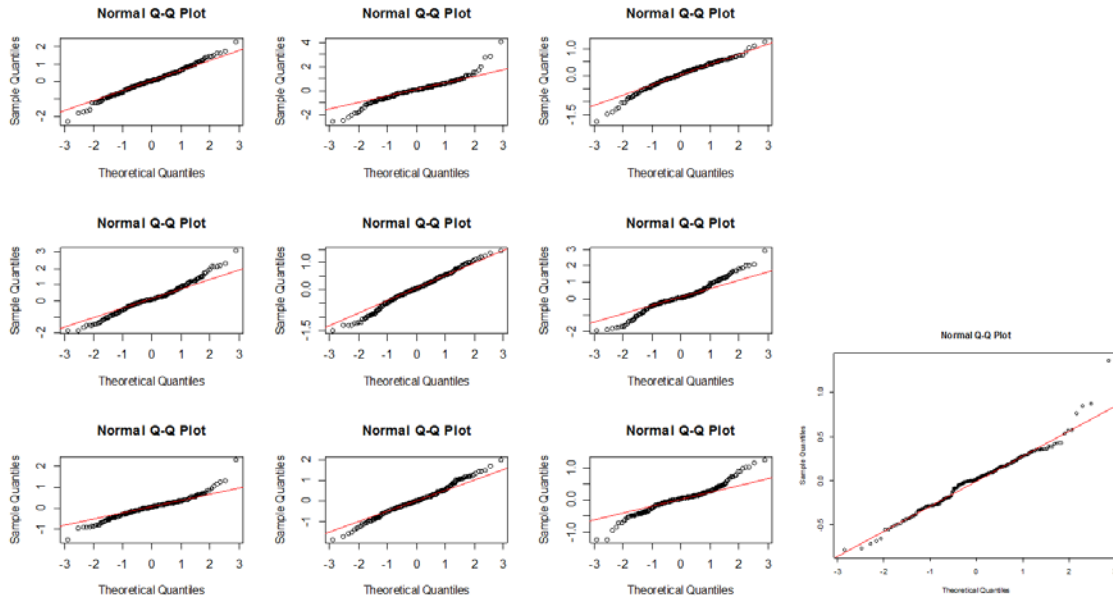


Fig. 11: W-NNAR performance curve of groundwater level in Rajshahi district

Table 4 shows the accuracy of the SARIMA estimation was verified by determining the following values: Mean error 0.423, Mean absolute error 4.820, Root mean squared error 6.490, Percentage error -8.74, Mean absolute percentage error 91.50 for original groundwater level of Baghmara upazila. The value of the average error should be close to zero. In this case, there is a slight underestimation. The MAE informs about the average aberrations of the actual realizations from the forecast ones for the forecasted variable in the period of forecast. The PE indicates what percentage of the actual realization of the forecast variable is the forecast error. The MAPE error should rather be used to compare models and should not be used to determine a single forecast error. Secondly, the SARIMA model was used. The autocorrelation diagram (ACF) and the partial autocorrelation graph - PACF were produced (Fig. 4).

**(i) Model identification**

The first step is to check whether there is any seasonality exists in the observed data and if the data is stationary. Time Series plot (Fig. 4) shows that there is a clear seasonality with periodicity of one year (twelve month) in the data set. The ACF (Autocorrelation Function) and PACF (Partial Autocorrelation Function) are significant in identifying stationary of the data set.

In order to fit an SARIMA model stationary data in both variance and mean are needed. Stationarity could be attained in the variance by having log transformation and differencing of the original data to attain stationarity in the mean. Since data series contain zero values straight forward log transformation is not possible. In this data series, a seasonal first difference (D = 1) of the original data was done in order to obtain stationarity. Thereafter, ACF and PACF for the differenced series were tested to check stationarity. The ACF and PACF (Fig. 4) show that one order seasonal differencing is adequate. Although further differencing shows a similar result but first seasonal differencing has a minimum standard deviation. Therefore, one order difference is enough for the data series. From this, a preliminary SARIMA (p, 1, q) × (P, 1, Q)<sub>12</sub> was selected.

**(ii) Model Estimation**

Since the orders P, p and Q, q necessary to adequately model for a given problem is not known to us. It is required to determine the model that best fits the data based on observing the ACF and the PACF of the differenced data. After carefully examining ACF and PACF, following five models were identified for test. These models are: SARIMA(3, 1, 2)(2,1, 2)<sub>12</sub>, SARIMA(2, 1, 2)(2,0,1)<sub>12</sub>, SARIMA(1,1,2)(2,1,1)<sub>12</sub>, (Fig. 8).

### **(iii) Model Diagnostic Checking**

Once the models have been fitted to the data, a number of diagnostic checks were initialized. If the model fits well, the residuals should be uncorrelated with constant variance. Moreover, in developing model this is often assumed that the errors are normally distributed. Hence, we expect the residuals to be more or less normally distributed.

Standard checks for SARIMA is to compute the ACF and the PACF of the residuals. Further diagnostics checking can be done by looking at the residuals in various ways (Fig.11). If the residuals are normally distributed, they should all more or less lie on a straight upward sloping line (Bowerman, and O'Connell, 1993).

### **(iv) Forecasting**

SARIMA(p, d, q) (P, D, Q)<sub>12</sub> was applied to forecast the monthly groundwater level data from January 1991 to December 2013. Forecasted values of January 2014 to December 2018 were used to compare the observed and forecasted values. The SARIMA accuracy of forecasted value for groundwater level shows Table 4, that is significant result. It is observed that measured monthly values fall within the error bound, and the forecasted track of the seasonal pattern fits reasonably well.

## **5.2 The NNAR results**

The autoregressive neural networks model (NNAR) estimation (training) methodology has been used. This algorithm is one of the most commonly used methods because of its valuable properties which are seen as having big advantages. In neural networks, there is no specific method to find the best design of the network. Thus, forecasts of the groundwater level in Rajshahi district with different parameter values have been examined, considering different number of hidden layers, and different lags. The researcher found that the minimum values of the RMSE, for the time series was 2.55 at 50 hidden layers and 12 lags.

Applying NNAR, the percentage of observations for training, which must have the same number of observations, 228 (January, 1991 to December, 2009), as we have in SARIMA for training is determined, so we have increased in a series of 48 (January, 2010 to December, 2013) observations for comparison in the prediction.

The learning rate assumed a continuous learning rate throughout the training. The performance of the algorithm is very sensitive to the proper setting for the learning rate. If you have chosen too high learning rate, the algorithm may oscillate and becomes unstable. If the selected learning rate is very small, the algorithm would take a long time to converge.

Selection of hidden layers need to experience more than the mathematical technique. When the number of hidden layers units is small, the correlation of the output and input cannot be studied well and the errors increase. Moreover, when the number of hidden layers units is more than adequate, even an unrelated noise can be studied as well as the correlation of both input and output, and the error increase accordingly.

There are some methods to get the number of hidden layer units; however, there is no general solution for this problem (Kermanhahi, et al, 2002). Therefore, we decided to start with one hidden layer and gradually increasing the number of hidden layers to a thirteen layers.

Wavelet transformation decomposed the time series into time - frequency space, enabling the identification of both the dominant modes of variability and how those modes vary with time. It identified significant variability (at the 95% confidence level) at an March-May month period from 1991 to 2013. Fig. 2 shows the wavelet decomposition of the groundwater level signal for the Rajshahi district. The signal wavelet is reconstructed using the approximation-and-detail process described above, and wavelet denoising is performed. Fig. 3 and 4 show the denoised signals of the groundwater level at the Rajshahi district, respectively. The red lines indicate the original signals, and the black lines indicate the denoised signals. Outliers and noise are removed from the denoised signal, but the trend is the same as in the original series; this is the main mechanism of wavelet denoising.

The augmented Dickey - Fuller (ADF) test was applied to test the unit root in the denoised groundwater level of the all upazila for different situations, such as in the presence of a drift, a drift and a linear trend, and no drift and a linear trend. Table 2 presents the ADF unit root test results for the original and 1<sup>st</sup> differenced series. The autocorrelation function (ACF) and partial autocorrelation function (PACF) are used to identify the order of the tentative model. The correlogram shows that the ACF has significant spikes at several lags, which display a periodic order over 12 months due to seasonal effects. The PACF also has significant spikes at several lags. Thus, the model may be a seasonal autoregressive integrated moving average (SARIMA) model. The least squares method is applied to estimate the parameter of the time series. For the groundwater level, the final candidate model for estimating the parameter is SARIMA (p, d, q) (P, D, Q)<sub>m</sub>. The estimated values, standard error, t-statistic and p-values for the SARIMA model are shown in Fig. 8. All coefficients for the estimated model are significant at the 5% level of significance. The R<sup>2</sup> value of the estimated model is 0.903, indicating

that approximately 90.3% of the variation in the monthly groundwater level can be explained by the estimated previous lag value and the lagged error terms. The  $R^2$  and adjusted  $R^2$  values suggest the goodness of fit of the model. The autocorrelation was evaluated using the Durbin-Watson (DW) test, and the results suggest that the estimated coefficients are free from autocorrelation problems because the DW value is approximately 2. The minimum values of the Akaike information criterion (AIC), Schwarz information criterion (SC) and Hannan-Quinn criterion (HQ) are also satisfactory. Fig. 8 shows that the fitted values nearly match the actual values and that the residuals do not vary significantly; thus, the fit is good. Hence, the final W-ARIMA models for the selected variables were chosen.

### **5.3 Comparison between W-ARIMA and W-NNAR results:**

Comparison is made between, the results obtained from applying both ARIMA and NNAR methods through looking at the results.

Can be easily note from the preceding table the RMSE of SARIMA model equivalent to 10 times RMSE of the NNAR model, this means that it is higher by 92.516 from NNAR model. Finally, we can conclude from the above dissuasion that the results of NNAR model are much better than the ARIMA model results and more efficient.

We can conclude from the above dissuasion that the results of NNAR model are much better than the ARIMA model results and more efficient.

## **VI. Conclusion**

A brief comparison among the sophisticated methods of forecast process was conducted proper validation. The forecast of groundwater level data is a complex process for several reasons. The most important reason encountered during this work is the fact that this series are usually very noisy. Excellent forecast performances were confirmed by the W-SARIMA model. The methods applied to the data of 9 upazilas and found to be consistently performed.

## **Reference**

- [1]. Adamowski, J. and H. F. Chan (2011). *A wavelet neural network conjunction model for groundwater level forecasting*. Journal of Hydrology **407**(1): 28-40.
- [2]. Adamowski, J. and K. Sun (2010). *Development of a coupled wavelet transform and neural network method for flow forecasting of non-perennial rivers in semi-arid watersheds*. Journal of Hydrology **390**(1): 85-91.
- [3]. Adamowski, J., Karapataki, C., 2010. *Comparison of multivariate regression and artificial neural networks for peak urban water-demand forecasting: evaluation of different ANN learning algorithms*. J. Hydrol. Eng. **15** (10), 729-743. [http://dx.doi.org/10.1061/\(ASCE\)HE.1943-5584.0000245](http://dx.doi.org/10.1061/(ASCE)HE.1943-5584.0000245).
- [4]. Adamowski, K., A. Prokoph and J. Adamowski (2009). *Development of a new method of wavelet aided trend detection and estimation*. Hydrological Processes **23**(18): 2686-2696.
- [5]. Box, G. E. P., G. M. Jenkins, G. C. Reinsel and G. M. Ljung (1976). *Time series analysis: forecasting and control*, John Wiley & Sons.
- [6]. Conraria, L. A. and M. J. Soares (2011). *The continuous wavelet transform: A primer*.
- [7]. Daliakopoulos, I. N., P. Coulibaly and I. K. Tsanis (2005). *Groundwater level forecasting using artificial neural networks*. Journal of Hydrology **309**(1): 229-240.
- [8]. Dong, Z., X. Guo, J. Zheng and L. Xu (2001). *Calculation of noise resistance by use of the discrete wavelets transform*. Electrochemistry communications **3**(10): 561-565.
- [9]. Faraway, J. and C. Chatfield (1998). *Time series forecasting with neural networks: a comparative study using the airline data*. Applied statistics: 231-250.
- [10]. Faruk, D. Ö. (2010). *A hybrid neural network and ARIMA model for water quality time series prediction*. Engineering Applications of Artificial Intelligence **23**(4): 586-594.
- [11]. Hyndman, R. J. and G. Athanasopoulos (2014). *Forecasting: principles and practice*, OTexts.
- [12]. Kim, T. W. and J. B. Valdés (2003). *Nonlinear model for drought forecasting based on a conjunction of wavelet transforms and neural networks*. Journal of Hydrologic Engineering **8**(6): 319-328.
- [13]. Kisi, O. and M. Cimen (2011). *A wavelet-support vector machine conjunction model for monthly stream flow forecasting*. Journal of Hydrology **399**(1): 132-140.
- [14]. Krishna, B., Y. Satyaji Rao and T. Vijaya (2008). *Modelling groundwater levels in an urban coastal aquifer using artificial neural networks*. Hydrological Processes **22**(8): 1180-1188.
- [15]. Mohammadi, K., H. Eslami and R. Kahawita (2006). *Parameter estimation of an ARMA model for river flow forecasting using goal programming*. Journal of Hydrology **331**(1): 293-299.
- [16]. Nalley, D., J. Adamowski, B. Khalil and B. Ozga-Zielinski (2013). *Trend detection in surface air temperature in Ontario and Quebec, Canada during 1967–2006 using the discrete wavelet transform*. Atmospheric Research **132**: 375-398.
- [17]. Nourani, V., M. T. Alami and M. H. Aminfar (2009). *A combined neural-wavelet model for prediction of Ligvanchai watershed precipitation*. Engineering Applications of Artificial Intelligence **22**(3): 466-472.
- [18]. Pal, S. and P. Devara (2012). *A wavelet-based spectral analysis of long-term time series of optical properties of aerosols obtained by lidar and radiometer measurements over an urban station in Western India*. Journal of Atmospheric and Solar-Terrestrial Physics **84**: 75-87.
- [19]. Parnell, A. C. (2013). *Climate Time Series Analysis: Classical Statistical and Bootstrap Methods*, Wiley Online Library.
- [20]. Pingale, S. M., D. Khare, M. K. Jat and J. Adamowski (2014). *Spatial and temporal trends of mean and extreme rainfall and temperature for the 33 urban centers of the arid and semi-arid state of Rajasthan, India*. Atmospheric Research **138**: 73-90.

- [21]. Rahman, M. J. and M. A. M. Hasan (2014). *Performance of wavelet transform on models in forecasting climatic variables*. Computational Intelligence Techniques in Earth and Environmental Sciences, Springer: 141-154.
- [22]. Ramana, R. V., B. Krishna, et al. (2013). *Monthly rainfall prediction using wavelet neural network analysis*. Water resources management **27**(10): 3697-3711.
- [23]. Reis, A. J. R. and A. P. A. Da Silva (2005). *Feature extraction via multi-resolution analysis for short-term load forecasting*. Power Systems, IEEE Transactions on **20**(1): 189-198.
- [24]. Singh, J., H. V. Knapp, et al. (2005). *Hydrological modeling of the iroquois river watershed using HSPF and SWAT1*, Wiley Online Library.
- [25]. Suryanarayana, C., C. Sudheer, V. Mahammood and B. K. Panigrahi (2014). *An integrated wavelet-support vector machine for groundwater level prediction in Visakhapatnam, India*. Neurocomputing **145**: 324-335.
- [26]. Team, R. C. (2014). *R: A language and environment for statistical computing*. R Foundation for Statistical Computing, Vienna, Austria. 2013, ISBN 3-900051-07-0.
- [27]. Wang, W. and J. Ding (2003). *Wavelet network model and its application to the prediction of hydrology*. Nature and Science **1**(1): 67-71.